

Measurement of elastic properties of kerogen

Fuyong Yan, De-hua Han*, Rock Physics Lab, University of Houston

Summary

To have good understanding of elastic properties of organic shale, it is fundamental to know the elastic properties of its mineral components. Kerogen is the most important component of organic shale, but information about its elastic properties is scarce. We have measured ultrasonic velocities on 9 laboratory isolated kerogen samples from Green River shale in Colorado. From data measured on both dry and saturated samples, we can invert the bulk modulus of kerogen using the Gassmann equation, Reuss bound and Voigt bound. The bulk modulus of kerogen is estimated to lie around 3.5-5 GPa. We have also argued that the shear modulus of kerogen is around half of the bulk modulus.

Sample description and molding

The process of isolating kerogen from source rocks is complicated and time consuming, thus kerogen samples are very precious. For some kerogen samples, only a very tiny amount (less than half of one gram) is available for ultrasonic measurement. The kerogen samples are mostly in the form of powder (Figure 1) and some are in the form of small chunks. The colors vary from brown to black. All the kerogen samples belong to Type I kerogen. These 9 samples are classified into two groups: five samples are brown and appear less oily, which seems to be in early maturation stage; the other four samples are in dark brown to black color and oily, which seems in later maturation stage as shown in Figure 2. And they are all from Green River basin, Colorado.

Measurement equipment and procedure

It is almost impossible to make ultrasonic velocity measurement on loose kerogen powder. The first step is to mold the kerogen powder into a cylindrical shape similar to a small core plug (Figure 2). Figure 3 shows the vase, cylindrical container and steel bullets used to mold the sample. The sample weight is measured by digital scale with resolution of 1 milligram. The sample length is controlled around 10 mm. The sample is stayed under compression state on vase overnight. Then the steel bullets are replaced with PEEK buffers and the sample is ready for ultrasonic velocity measurement.

Both P-wave and S-wave velocities are measured on dry samples under axial pressure from 2860 psi to 286 psi. The pressure is controlled by the gas regulator. Lateral pressure is generated by the confined vessel without control. Due to



Figure 1: Kerogen powder



Figure 2: Molded kerogen samples (diameter=9.55mm)

the ductile behavior of kerogen, we believe that the lateral stress will be close to the axial stress. We have to be careful to apply the pressure with the same procedure and wait for stability before signal recording. The sample length change is monitored with a digital caliper at each pressure step. After dry velocity measurement, the kerogen sample is vacuumed and then distilled water is pumped into the sample. After 1-4 hours of saturation the ultrasonic signal is stabilized (with advanced time and much higher amplitude of the first arrival) and full saturation condition is assumed to be reached. The axial pressure is first increased to 2860 psi and then decreased to 572 psi by step of 286 psi. The pore pressure is controlled by a digital pump at 286 psi. After ultrasonic measurement on saturated kerogen sample, the kerogen sample is taken out carefully to keep the cylindrical form. The saturated sample is weighed again after wiping quickly away the water drops on the sample surface using paper towel (This water are from pore pressure lines). This is for gross estimation of the porosity of the kerogen sample: weight difference between dry and

Kerogen elastic properties



Figure 3: Molding of kerogen sample

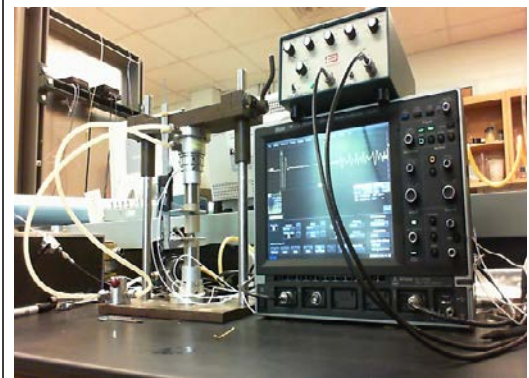


Figure 4: Ultrasonic velocity measurement setup

saturated sample is the weight of pore fluid water, which can be used to estimate pore volume. After weighting, the saturated sample is put into oven to dry for 24 hours at 40-50 °C. The dried sample is weighted again to check whether water is completely driven out by evaporation. Then, we measured grain density of dry samples using helium porosimeter. With measured bulk volume of the core sample, we can calculate porosity. The porosimeter porosities are generally consistent with those estimated from weight of pore fluid water.

Sensitivity analysis

Our primary goal is to estimate the bulk modulus of kerogen from velocity measurement on both dry and fully saturated conditions using the Gassmann equation (Gassmann, 1951).

$$K_{\text{sat}} = K_{\text{dry}} + \frac{n^2}{\frac{n-\phi}{K_m} + \frac{\phi}{K_f}} \quad (1)$$

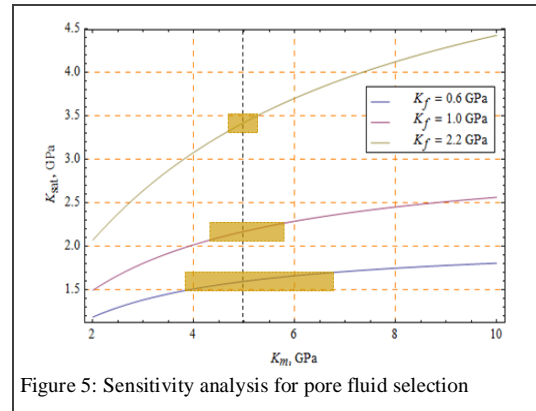


Figure 5: Sensitivity analysis for pore fluid selection

Where n is Biot coefficient ($n = 1 - \frac{K_{\text{dry}}}{K_m}$), K_m is the bulk modulus of kerogen, K_{sat} and K_{dry} are effective bulk moduli of fully saturated and dry kerogen sample respectively, and K_f is pore fluid bulk modulus.

From laboratory measurement and modeling, we know that Gassmann equation usually apply very well for porous rock (Han and Batzle, 2004; Yan and Han, 2011), and it is reasonable to assume that the Gassmann equation should also apply well for the kerogen samples. The process of estimating K_m is basically to invert K_m from the saturation effect using Gassmann equation. The saturation effect can be approximated by product of the gain function ($G(\phi)$) and pore fluid bulk modulus (Han and Batzle, 2004):

$$K_{\text{sat}} \approx K_{\text{dry}} + G(\phi)K_f = K_{\text{dry}} + \frac{n^2}{\phi}K_f \quad (2)$$

In order to invert K_m reliably from K_{sat} , it is critical to select a pore fluid that makes K_{sat} be sensitive to K_m . Here we test how K_{sat} correlates to K_m with different pore fluids with bulk modulus of 0.6, 1.0, 2.2 GPa, which approximately correspond to butane, oil and distilled water respectively under room temperature and 500 psi pressure conditions.

Figure 5 shows that K_{sat} is more sensitive to K_m when water is selected as pore fluid. Uncertainty of 0.2 GPa in estimating K_{sat} corresponds to uncertainty of 0.5 GPa (~10%) in inverting K_m . If we use butane as saturation fluid, for the same uncertainty in estimating K_{sat} , the uncertainty in inverting K_m will be 3 GPa (~60%), which is too large to be acceptable. Thus, water is the best option for saturation fluid comparing to butane and oil.

Measurement results and analysis

Kerogen elastic properties

Figure 6 shows measured velocities for two kerogen samples with grain density 1.13 and 1.29 g/cm³ respectively. It can be seen that for both samples velocities are not sensitive to the differential pressure when it is higher than 1500 psi. The saturation effect for both samples are significant. The P-wave velocity of fully saturated samples can be as high as 1.9 km/s in comparison to 1.1 km/s of dry sample. The sample with lower porosity has stronger saturation effect. We failed to pick up the first arrivals for S-wave signal of saturated samples. Figure 7 show the estimated bulk modulus of kerogen for these two samples. Along with K_m inverted by Gassmann equation, we also plotted the K_m inverted by Reuss bound and Voigt bound.

$$\frac{1}{K_{sat}} = \frac{1-\phi}{K_m} + \frac{\phi}{K_f} \quad (3)$$

$$K_{sat} = (1-\phi)K_m + \phi K_f \quad (4)$$

If there is no measurement error, the inverted K_m by Reuss bound is the highest possible value for K_m and the inverted K_m by Voigt bound is the lowest possible value for K_m . The relative small difference between K_m inverted by Reuss bound and that inverted by Voigt bound shows that uncertainty due to rock physical model is not significant.

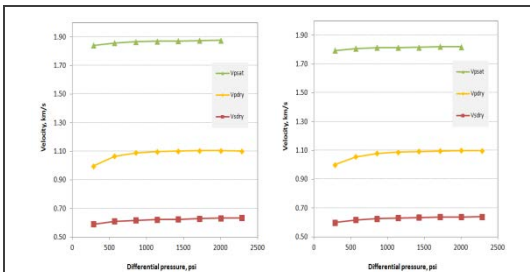


Figure 6: Velocity data for kerogen samples(Left: $\rho_M = 1.13 \text{ g/cm}^3$, $\phi \approx 28.2\%$; Right: $\rho_M = 1.29 \text{ g/cm}^3$, $\phi \approx 37.1\%$)

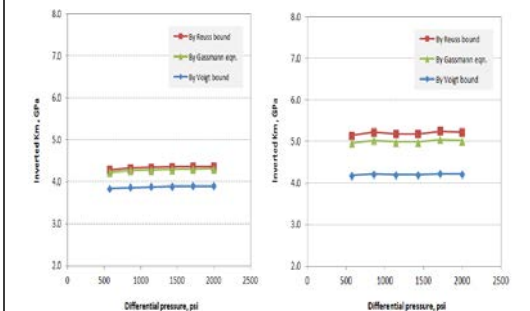


Figure 7: Estimated kerogen bulk modulus for the kerogen samples in Fig. 6.

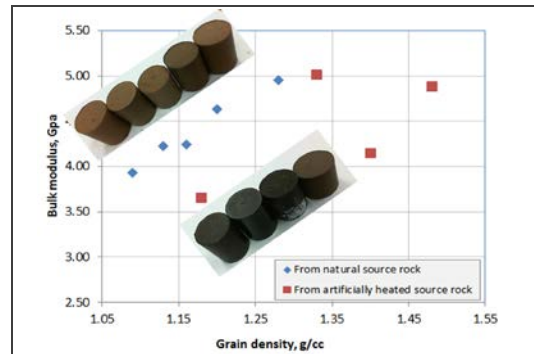


Figure 8: Inverted bulk modulus using Gassmann equation for all the Kerogen samples

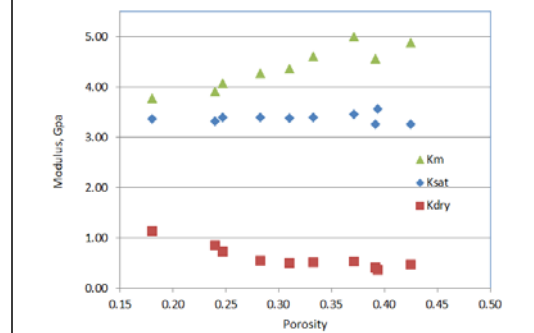


Figure 9: Kerogen sample porosity and bulk modulus

The smaller is the kerogen modulus, the smaller is the difference. This corroborate with previous sensitivity analysis that more reliability in inverting K_m can be achieved by using pore fluid of relatively big bulk modulus(the closer is the pore fluid bulk modulus to that of kerogen, the less is the uncertainty). It is reasonable and expected that the inverted K_m values don't have trend varying with differential pressure.

Figure 8 shows the inverted K_m using Gassmann equation for all the kerogen samples. The bulk modulus of kerogen ranges between 3.5-5.0 GPa. For less matured kerogen samples, there is an obvious trend that bulk modulus of kerogen increases with grain density. The more matured kerogen samples generally have higher grain density, but the bulk modulus does not necessarily increases. The overlaid two groups of images of kerogen samples are both aligned by grain density (increasing from bottom left to top right).

Figure 9 shows cross plots of the sample porosity with bulk modulus. During sample molding and measurement, all the samples experienced similar compaction history, but some samples has much higher porosity (43%) and some sample has much lower porosity(18%). The maximum pressure

Kerogen elastic properties

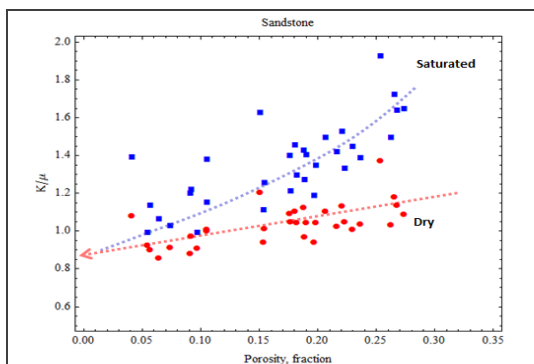


Figure 10: Relation between K/μ and porosity for sandstone (Han's data, 1986)

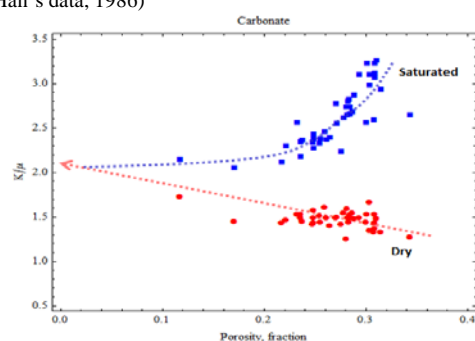


Figure 11: Relation between K/μ and porosity for carbonate (UH RPL)

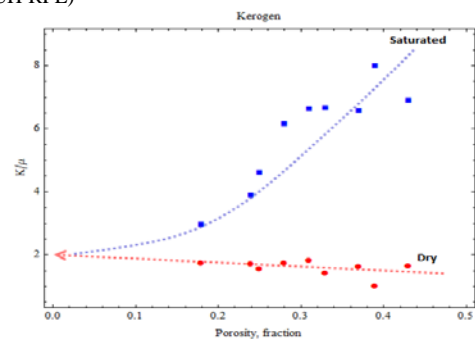


Figure 12: Speculation of K/μ ratio of kerogen

load is about 3000 psi. From experience of loose sands compaction, even under high pressure of 10000 psi, porosity less than 40% is very difficult to be achieved. Also from Figure 9, the lower the kerogen bulk modulus, the lower is sample porosity. The low porosity of kerogen sample may be related to plastic property of kerogen, which may explain why kerogen is often in lenticular shape (Vernik and Milovac, 2011) in the earth's gravity field and kerogen content has good correlation with shale anisotropy (Vernik and Nur, 1992; Yan et al., 2012).

We cannot estimate shear modulus of kerogen using above procedure, but we can speculate K/μ ratio of kerogen using available information. Figure 11 shows correlation between K/μ ratio with porosity for both dry and saturated sandstone rocks. With decrease of porosity, the K/μ ratio for both dry rock and saturated rock decreases toward the "mineral point", which is K_m/μ_m of the sandstone rock matrix, usually around 0.9 for clean sandstone. Figure 11 shows correlation between K/μ ratio with porosity for both dry and saturated limestone rocks (RPL data). With decrease of porosity, the K/μ ratio for dry rock increases and the K/μ ratio for saturated rock decreases, and they both point toward the "mineral point" or "matrix point", which is K_m/μ_m of limestone mineral, usually around 2.1.

Similarly, we can also plot the K/μ of kerogen samples under both saturated and dry conditions against porosity, as show in Figure 12. It can be seen that K/μ of kerogen samples behave more like carbonate rocks: the K/μ of dry kerogen samples have a slight trend of increasing with decreasing porosity, while the K/μ of saturated kerogen samples decreases with porosity. The K/μ ratio for both dry and saturated cases points toward the mineral point (K_m/μ_m) around 2.0. Thus we speculate that the shear modulus of kerogen is about half of the bulk modulus.

Conclusions

We have estimated that the bulk modulus of kerogen in Green River area lies around 3.5—5.0 GPa. For kerogen from the same area, the bulk modulus of kerogen have a trend to increase with kerogen density. After artificial heating, the kerogen grain density increases but the bulk modulus may not increase. We have speculated that the shear modulus of kerogen is half of bulk modulus.

Acknowledgements

We would like to thank the Geochemical Laboratory of University of Houston to provide the kerogen samples in this study. Authors also thank our colleagues Qiuliang Yao and Min Sun for help in equipment setup and discussion. Also we would like to thank the Fluid/DHI consortium sponsors for their financial support.

<http://dx.doi.org/10.1190/segam2013-1319.1>

EDITED REFERENCES

Note: This reference list is a copy-edited version of the reference list submitted by the author. Reference lists for the 2013 SEG Technical Program Expanded Abstracts have been copy edited so that references provided with the online metadata for each paper will achieve a high degree of linking to cited sources that appear on the Web.

REFERENCES

- Gassmann, F., 1951, On elasticity of porous media : Classics of elastic wave theory: SEG.
- Han, D.-H., 1986, Effects of porosity and clay content on acoustic properties of sandstones and consolidated sediments: Ph.D. thesis, Stanford University.
- Han, D.-H., and M. L. Batzle, 2004, Gassmann's equation and fluid saturation effects on seismic velocities: *Geophysics*, **69**, 398–405, <http://dx.doi.org/10.1190/1.1707059>.
- Mavko, G., T. Mukerji, and J. Dvorkin, 1998, *The rock physics handbook*: Cambridge University Press.
- Reuss, A., 1929, Berechnung der Fließgrenzen von Mischkristallen auf Grund der Planstizitättsbedingung für Einkristalle : *Zeitschrift für : Angewandte Mathematik und Mechanik*, **9**, no. 1, 49–58, <http://dx.doi.org/10.1002/zamm.19290090104>.
- Yan, F., D.-H. Han, and Q. Yao, 2012, Oil shale anisotropy measurement and sensitivity analysis: Presented at the 82nd Annual International Meeting, SEG.
- Vandenbroucke, M., and C. Largeau, 2007, Kerogen origin, evolution and structure: *Organic Geochemistry*, **38**, no. 5, 719–833, <http://dx.doi.org/10.1016/j.orggeochem.2007.01.001>.
- Vernik, L., and J. Milovac, 2011, Rock physics of organic shales: *The Leading Edge*, **30**, 318–323, <http://dx.doi.org/10.1190/1.3567263>.
- Vernik, L., and A. Nur, 1992, Ultrasonic velocity and anisotropy of hydrocarbon source rocks: *Geophysics*, **57**, 727–735, <http://dx.doi.org/10.1190/1.1443286>.